Accepted Manuscript

Development of bioactive gemcitabine-D-Lys^6-GnRH prodrugs with linker-controllable drug release rate and biopharmaceutical profile

Nisar Sayyad, Eirinaios I. Vrettos, Theodoros Karampelas, Christos M. Chatzigiannis, Katerina Spyridaki, George Liapakis, Constantin Tamvakopoulos, Andreas G. Tzakos

PII: S0223-5234(19)30051-0

DOI: https://doi.org/10.1016/j.ejmech.2019.01.041

Reference: EJMECH 11048

To appear in: *European Journal of Medicinal Chemistry*

Received Date: 20 November 2018

Revised Date: 16 January 2019

Accepted Date: 17 January 2019

Please cite this article as: N. Sayyad, E.I. Vrettos, T. Karampelas, C.M. Chatzigiannis, K. Spyridaki, G. Liapakis, C. Tamvakopoulos, A.G. Tzakos, Development of bioactive gemcitabine-D-Lys^6-GnRH prodrugs with linker-controllable drug release rate and biopharmaceutical profile, *European Journal of Medicinal Chemistry* (2019), doi: https://doi.org/10.1016/j.ejmech.2019.01.041.

Development of bioactive gemcitabine-D-Lys^{6}-GnRH prodrugs with linker-controllable drug release rate and biopharmaceutical profile

Nisar Sayyad[1], Eirinaios I. Vrettos[1], Theodoros Karampelas[2], Christos M. Chatzigiannis[1], Katerina Spyridaki[3], George Liapakis[3], Constantin Tamvakopoulos[2], Andreas G. Tzakos[1*]

[1]Department of Chemistry, Laboratory of Chemical Biology, University of Ioannina, Ioannina, GR-45110, Greece;
[2]Center of Clinical Research, Experimental Surgery and Translational Research, Biomedical Research Foundation Academy of Athens (BRFAA), Soranou Ephessiou Street 4, Athens GR-11527, Greece;
[3]Department of Pharmacology, Faculty of Medicine, University of Crete, Heraklion, Crete, Greece

Highlights

- 3 different peptide-drug conjugates (PDCs) targeting the GnRH-R were synthesized
- The impact of the linker was explored in terms of PDCs stability and bioactivity
- Binding affinity of PDCs to GnRH-R was enhanced with respect to GnRH-II
- PDCs showed amplified plasma stability and pharmaceutical profile

Graphical Abstract

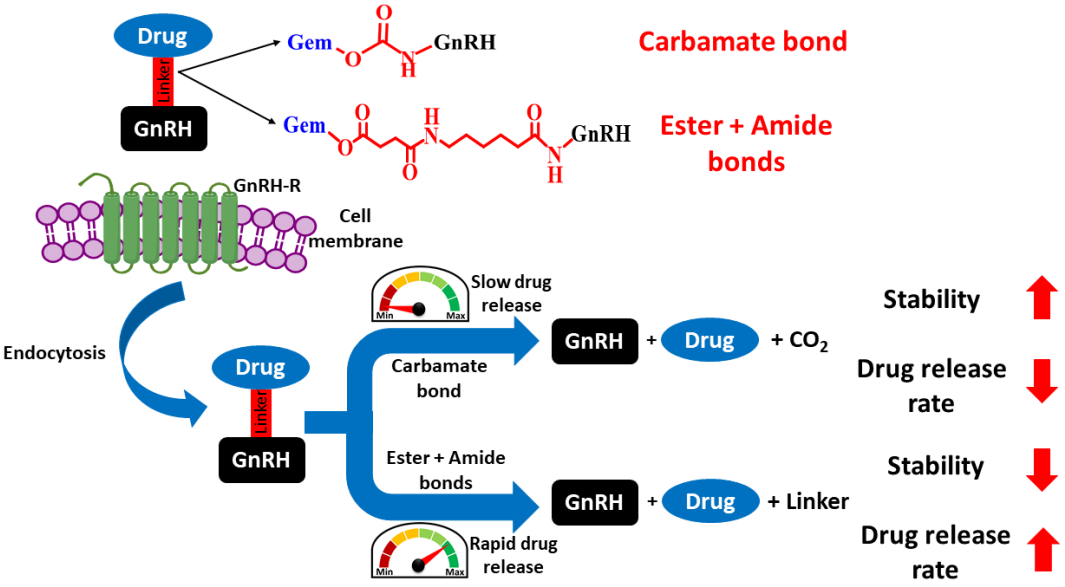

Abbreviations

GnRH, Gonadotropin Releasing Hormone; GnRH-R, Gonadotropin Releasing Hormone-Receptor; dFdC, 2'-2'difluorodeoxycytidine; dFdU, 2, 2'-difluorodeoxyuridine; n-BuOH (n-butanol); MeCN, acetonitrile; HATU, 1-[Bis(dimethylamino)methylene]-1H-1,2,3-triazolo[4,5-b]pyridinium 3-oxid hexafluorophosphate; DIPEA, N,N-Diisopropylethylamine; PDC, Peptide-Drug Conjugate; EGFR, Epidermal Growth Factor Receptor;

Abstract

Peptide-drug conjugates have emerged as a potent approach to enhance the targeting and pharmacokinetic profiles of drugs. However, the impact of the linker unit has not been explored/exploited in depth. Gemcitabine (dFdC) is an anticancer agent used against a variety of solid tumours. Despite its potency, gemcitabine suffers mostly due to its unspecific toxicity, lack of targeting and rapid metabolic inactivation. To minimize these limitations and enable its targeting to tumours overexpressing the GnRH receptor, we examined the peptide-drug conjugation approach. Our design hypothesis was driven by the impact that the linker unit could have on the peptide-drug conjugate efficacy. Along these lines, in order to exploit the potential to manipulate the potency of gemcitabine through altering the linker unit we constructed

three different novel peptide-drug conjugates assembled of gemcitabine, the tumour-homing peptide D-Lys^6-GnRH and modified linker building blocks. Specifically, the linker was sculpted to either allow slow drug release (utilizing carbamate bond) or rapid disassociation (using amide and ester bonds). Notably, the new analogues possessed up to 95.5-fold enhanced binding affinity for the GnRH receptor (GnRH-R) compared to the natural peptide ligand D-Lys^6-GnRH. Additionally, their *in vitro* cytotoxicity was evaluated in four different cancer cell lines. Their cellular uptake, release of gemcitabine and inactivation of gemcitabine to its inactive metabolite (dFdU) was explored in a representative cell line. *In vitro* stability and the consequent drug release were evaluated in cell culture medium and human plasma. *In vivo* pharmacokinetic studies were performed in mice, summarizing the relative stability of the three conjugates and the released levels of gemcitabine in comparison with dFdU. These studies suggest that the fine tuning of the linkage within a peptide-drug conjugate affects the drug release rate and its overall pharmaceutical profile. This could eventually emerge as an intriguing medicinal chemistry approach to optimize bio-profiles of prodrugs.

Keywords: Gemcitabine; Peptide-drug conjugate; Pharmacokinetics; Stability; Binding affinity;

1. Introduction

The menace of cancer is affecting humanity with rapidly increasing rate and is tending to become the number one cause of mortality worldwide. Therefore, cancer has turned into a top priority for the scientific community which is continuously attempting to unscramble its mechanism of action and discover new effective therapies or improve the existing ones. In this frame, an immense variety of drug-designing approaches has been developed, with the aim to improve conventional chemotherapy through alleviation of severe side-effects caused by collateral toxicity in healthy tissues [1]. This intriguing goal can be achieved through selective delivery of cytotoxic agents to tumour cells by conjugating chemotherapeutic agents with peptides [2-5] which selectively bind to cell surface proteins/receptors uniquely expressed or over-expressed in cancer cells (e.g. GnRH-R, EGFR, integrin receptors)

[6, 7]. Two peptide-drug conjugates (PDCs) have reached up to Phase-III clinical trials typify this class of chemotherapeutics [8, 9].

In peptide-drug conjugates, bioconjugation is achieved through linkers which may consist of a wide range of functional groups and therefore result in various bond formations like amide, ester, oxime, carbamate etc. These linker units could have a tremendous impact in the bioactivity profile of PDCs since they could instruct on the time that a drug will be released [10-12]. Furthermore, they have to be carefully designed for tethering the transporting vehicle to the cytotoxic warhead so as not to perturb the binding affinity of the tumour-homing peptide to its receptor [4].

Interestingly, the carbamate unit has been included, as a structural moiety, in many approved drugs/prodrugs including XP13512 [13] (a novel prodrug of gabapentin), capecitabine and 5-fluorouracil (5-FU) [14]. Carbamate moiety is often rationally selected to form drug-target interactions with certain receptors [15, 16] as also are often manipulated for use in the design of drugs and prodrugs to offer adequate systemic hydrolytic stability and enhanced overall bioavailability [17-20]. In specific, aliphatic amine-derived carbamates are known to be sufficiently stable and undergo hydrolytic degradation at a suitable rate for releasing the active drug [16, 21]. Intriguingly, this unit is frequently referred as a traceless linker, due to the fact that after its hydrolysis, the only by-product produced is gas CO_2 along with the starting amine and alcohol [22, 23].

Nucleoside analogues constitute a major class of chemotherapeutic agents administered to patients with progressed cancer. They are a part of a larger family of anticancer drugs known as antimetabolites, including pyrimidine and purine nucleoside derivatives with cytotoxic activity against various solid tumours [24]. Gemcitabine (2’ – deoxy – 2’, 2’ - difluorocytidine), a potent antimetabolite drug, is known to be active against several solid tumour types [25] and has gained FDA-approval for treating non-small cell lung, ovarian, bladder, pancreatic and breast cancer. Gemcitabine enters the cells through nucleoside transporters and immediately undergoes intracellular sequential conversion into the monophosphate (dFdCMP), diphosphate (dFdCDP) and finally triphosphate (dFdCTP) form [26]. The main mechanism of action of gemcitabine relies on the formation of dFdCTP, which replaces deoxycytidine during DNA replication and leads to cell death [27] and to a lesser extent on the formation of dFdCDP which interferes with thymidylate synthase that normally catalyzes the conversion of uridine monophosphate into thymidine

monophosphate [28]. However, gemcitabine is prone to certain limitations: i) it suffers from rapid metabolic inactivation to its metabolite dFdU through deamination either by cytidine deaminase (CDA) or by deoxycytidylate deaminase (DCTD), resulting in the monophosphorylated form of dFdU (dFdUMP) [28]; ii) cancer cells acquire drug resistance after extensive usage of gemcitabine, mostly by diminishing the expressed nucleoside transporters that facilitate the internalization of the drug [29, 30]; iii) it is indiscriminately toxic, affecting both cancer and healthy tissues and consequently result in severe side effects on patient's health [31].

The limitations of gemcitabine motivated us to design novel analogues with enhanced pharmacological properties and stability. Veltkamp et. al. has proved that prolonged administration of gemcitabine in patients with pancreatic cancer resulted in elevated intracellular levels of dFdCTP and higher overall toxicity in comparison with the standard infusion protocol [32]. Intrigued by these results, along with similar carbamate-based prodrugs of gemcitabine [33-35], we rationally designed and synthesized three novel peptide drug conjugates of gemcitabine (**Scheme 1**), consisting of either one traceless carbamate bond (small linker; compounds designated **2G$_1$** and **2G$_2$**) or two amide bonds and one ester bond (long linker; compound designated **GSHG**) tethering the drug and the tumour homing D-Lys^6-Gonadotropin Releasing Hormone (D-Lys^6-GnRH). The short linker (carbamate bond) has been included in the design since it can offer stability to a bioconjugate by decreasing the drug release rate (slow release), whereas the long linker consisted of a mixture of amide and ester bonds, could offer a rapid disassociation and a consequent faster drug release as these bonds are prone to intracellular esterases and amidases.

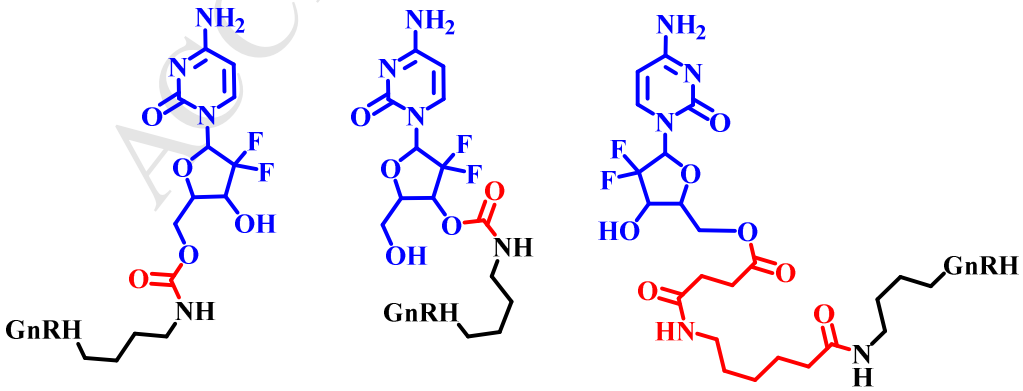

2G$_1$ **2G$_2$** **GSHG**

Scheme 1. Architecture of the three peptide-drug conjugates (D-Lys^6-GnRH-gemcitabine) where the different building blocks are highlighted (gemcitabine in blue, linkers in red and D-Lys^6-GnRH in black).

The **2G$_1$**, **2G$_2$** and **GSHG** peptide-drug conjugates have been designed with different linker building blocks in order to afford different hydrolytic stabilities and possibly might illustrate different potency. Specifically, **2G$_1$** and **2G$_2$** are expected to be more stable, enabling slow release of the cytotoxic agent, while compound **GSHG** is expected to afford rapid release of the cytotoxic agent.

The new analogues were evaluated regarding their binding affinity to the GnRH-R compared to D-Lys^6-GnRH. The stability and the intracellular concentrations of the conjugates, gemcitabine and dFdU were also explored *in vitro* in cell culture and plasma, as also *in vivo* in mice plasma.

2. Results and discussion

2.1 Design of D-Lys^6-GnRH-gemcitabine conjugates

In our former studies [3], we reported the conjugation of gemcitabine and D-Lys^6-GnRH peptide via hemiglutarate and hemisuccinate linkers. These conjugates, although are potent *in vitro* and in clinically relevant prostate cancer models, resulted in low hydrolytic stability and consequent high levels of both dFdC and dFdU. The results highlighted the dominant role of the linker towards the bioactive profile of each compound. Based on these findings, we aimed to explore and exploit linker's impact towards the biopharmaceutical profile of the final PDCs. We thus synthesized three peptide-drug conjugates bearing either a long linker (**GSHG**) or a very short traceless carbamate linker (**2G$_1$** and **2G$_2$**). Among a wide variety of classic bonds, we adopted carbamate due to its facile implementation and its hydrolytic stability offering a sporadic drug release.

Gemcitabine contains two hydroxyl functionalities, a primary 5'-OH and a secondary 3'-OH, which can be easily and rapidly conjugated with a tumour-targeting peptide (**Scheme 2**). Specifically, compound **4** was synthesized according to our previously reported synthetic scheme [3], while compound **3** was synthesized by reacting the ε-amino group of D-Lys^6-GnRH and the free carbonyl group of the previously Boc- protected ε-aminocaproic acid [36] with the usage of HATU as a coupling reagent. We would like to highlight here that, as we discovered recently, 1

eq. of HATU has to be used in order to avoid formation of unwanted side-products [37]. The ε-amine of compound **3** reacted with the free carboxylic acid of compound **4,** utilizing again 1 eq. of HATU as a coupling reagent, resulting to the relevant Boc-protected compound. Another Boc- deprotection step under acidic conditions was necessary to afford the final compound **GSHG**.

Compounds **2G$_1$** and **2G$_2$**, bearing carbamate bonds, were synthesized by reacting the ε-amino group of D-Lys^6-GnRH with the activated intermediates **2a** and **2b** respectively, followed by Boc- deprotection under acidic conditions (**Scheme 3**). Specifically, gemcitabine was selectively Boc- protected to afford compounds **1a** and **1b** [38], which were sequentially activated with the usage of bis(4-nitrophenyl)carbonate to afford the intermediates **2a** and **2b**, respectively. Intermediates **2a** and **2b** were treated with D-Lys^6-GnRH, with the usage of HATU as a coupling reagent, resulting in the final compounds **2G$_1$** and **2G$_2$**.

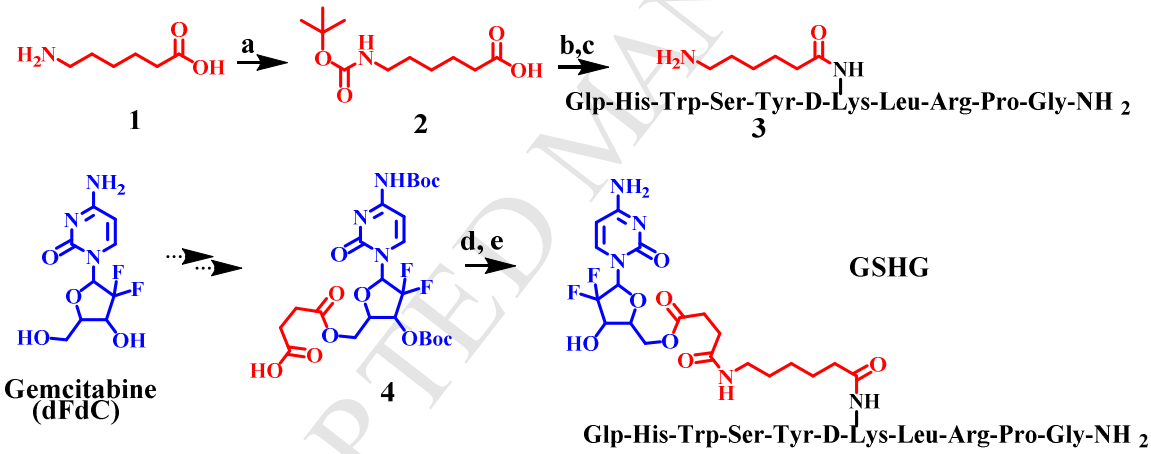

Scheme 2. Synthesis of **GSHG**. Reagents and conditions: **a)** Boc_2O, NaOH, Dioxane:Water, rt, 6h; **b)** D-Lys^6-GnRH, HATU, DIPEA, DMF, rt, 12h; **c)** TFA/H_2O/TIS (9.5/0.25/0.25, v/v), rt, 4h; **d) 3**, HATU, DIPEA, DMF, rt, 12h; **e)** TFA/ H_2O/ TIS (9.5/0.25/0.25, v/v), rt, 4h.

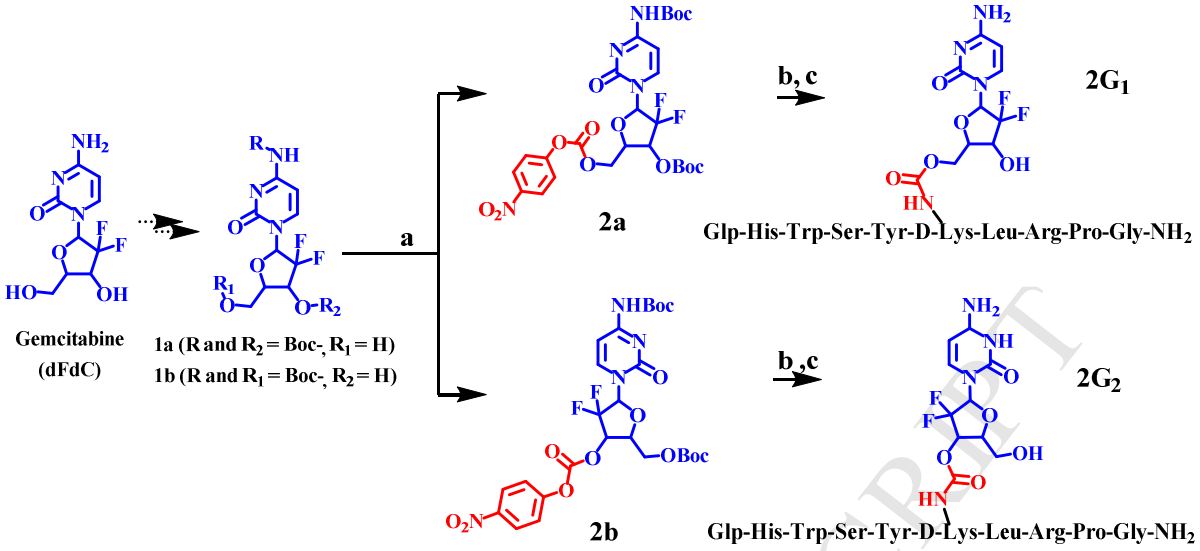

Scheme 3. Syntheses of the carbamate-based **2G$_1$** and **2G$_2$**. Reagents and conditions: **a)** Bis(4-nitrophenyl)carbonate, DIPEA, MeCN, rt, 6h; **b)** D-Lys^6-GnRH, DIPEA, DMF, rt, 12h; **c)** TFA/ H_2O/ TIS (9.5/0.25/0.25, v/v), rt, 4h.

2.2 Binding affinity towards human GnRH-R

The three synthesized conjugates (**2G$_1$**, **2G$_2$** and **GSHG**) were evaluated with respect to their binding affinity to the GnRH-R as shown in **Table 1**.

Table 1. Binding assay values IC_{50} (nM) of **2G$_1$**, **2G$_2$** and **GSHG** compared to native peptide ligand D-Lys^6-GnRH to GnRH-R.

Compounds	Radioligand Binding assay IC_{50} (nM)
2G$_1$	0.69 ± 0.02 nM
2G$_2$	0.11 ± 0.00 nM
GSHG	2.40 ± 0.04 nM
D-Lys^6-GnRH	10.5 ± 0.2 nM

The presented data show that **2G$_2$**, **2G$_1$** and **GSHG** bind to GnRH-R with 95.5-, 15.2-, and 4.4-fold higher affinity, respectively, than that of the native peptide D-Lys^6-GnRH (10.5 ± 0.2 nM, according to our former study [3]). When compared to our previously published compound **GSG** (IC_{50} = 7.1 ± 0.2 nM, according to our former study [3]), these three new conjugates presented enhanced binding affinity for the GnRH-R (65-, 10.3-and 3-fold higher binding affinity for **2G$_2$**, **2G$_1$** and **GSHG**, respectively). The latter can be attributed to the fact that the carbamate group is a

moiety of medium polarity, capable of forming hydrogen bonds as donor and acceptor through the peptide amide backbone [39] and thus adjusting inter- and intramolecular interactions with the targeted receptor(s). Also, the carbamate moiety induces a degree of conformational restriction due to the delocalization of nonbonded electrons on nitrogen into the carboxyl moiety [16] that could further favor the conformational entropy upon binding.

2.3 GnRH-gemcitabine conjugates exhibit antiproliferative potential *in vitro*. The antiproliferative effect of the three GnRH-gemcitabine analogues was evaluated in two androgen prostate cancer cell lines (DU145 and PC3) and in two breast cancer cell lines (MDA-MB-21 and MCF-7) using gemcitabine and D-Lys^6-GnRH as their corresponding controls as shown in **Table 2**. **GSHG** possesses the highest cytotoxic effect among the three conjugates, which is comparable with that of gemcitabine in the examined cell lines and especially regarding MCF-7 cells. Results are summarized in **Table 2** below:

Table 2. Antiproliferative effect (IC_{50} values in nM) of GnRH-gemcitabine conjugates compared with gemcitabine and D-Lys^6-GnRH in various cancer cell lines (DU145, PC3, MDA-MB-231, MCF-7).

Cell lines	**IC_{50} (nM)**				
	GSHG	**$2G_1$**	**$2G_2$**	**Gemcitabine**	**D-Lys^6-GnRH**
DU145	684 ± 203 (n=3)	>40,000 (n=3)	9,761 ± 6278 (n=3)	213 ± 40 (n=3)	>40,000 (n=3)
PC3	937 ± 228 (n=3)	>40,000 (n=3)	>40,000 (n=3)	416 ± 13 (n=3)	>40,000 (n=3)
MDA-MB-231	2,387 ± 1,220 (n=3)	>40,000 (n=3)	>40,000 (n=3)	1,567 ± 757 (n=5)	>40,000 (n=3)
MCF-7	55.5 ± 7.2 (n=3)	621.3 ± 113 (n=3)	449.1 ± 87.0 (n=3)	38.0 ± 14.1 (n=3)	>40,000 (n=3)

From the results presented above, it can be concluded that conjugates **2G$_1$** and **2G$_2$** bear less cytotoxicity in general when compared with the other compounds. This could be correlated with the high proteolytic stability of the conjugates, which results in an insufficient release of gemcitabine, associated with less toxicity. In order to verify this hypothesis, the three conjugates were subjected to stability studies in cell culture medium, as well as human plasma.

2.4 Stability studies and release of free gemcitabine in cell culture medium.

In **Figure 1A**, the degradation of the three conjugates over time is illustrated. Analogues bearing the carbamate bond (**2G$_1$** and **2G$_2$**) appeared to possess similar stability in the cell culture (stable even after 72 h), while analogue **GSHG** degraded fully in less than 24 h. In **Figure 1B**, the amounts of gemcitabine released from the three conjugates over time are presented.

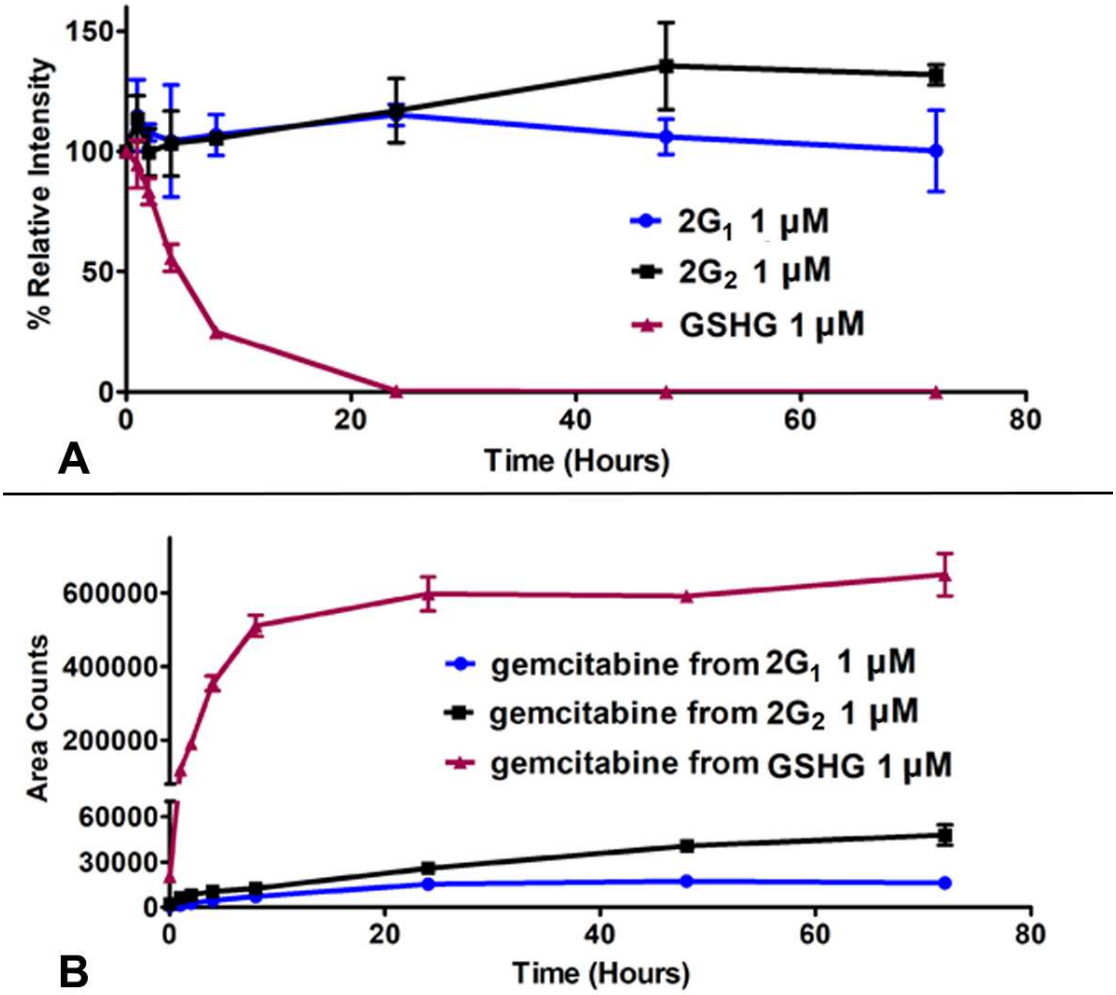

Figure 1. Stability of the three conjugates (**2G$_1$**, **2G$_2$** and **GSHG**) over time in cell culture medium (A) and release of gemcitabine (B).

The data presented in **Figure 1B**, fully correlate with the stabilities of the corresponding conjugates in cell culture medium, presenting low stability of **GSHG** which results in higher drug release. In contrast, the high stability of **$2G_1$** and **$2G_2$** results in low amounts of free gemcitabine.

These findings provide a rationale on the reduced cytotoxicity of **$2G_2$** and **$2G_1$** and the enhanced cytotoxicity of **GSHG**.

2.5 Stability studies of the GnRH-gemcitabine conjugates in human plasma.

To further understand the cell culture stability results, we performed stability experiments in human plasma, a more clinically relevant system. The corresponding analogues possess similar stabilities with those observed in cell culture medium. **Figure 2A** clearly demonstrates the enhanced stability of conjugates **$2G_1$** and **$2G_2$**, while in contrast conjugate **GSHG** degrades within 4 h. Likewise before, in **Figure 2B** are presented the levels of gemcitabine released by the three conjugates, which correlate with the stability pattern of **Figure 2A**.

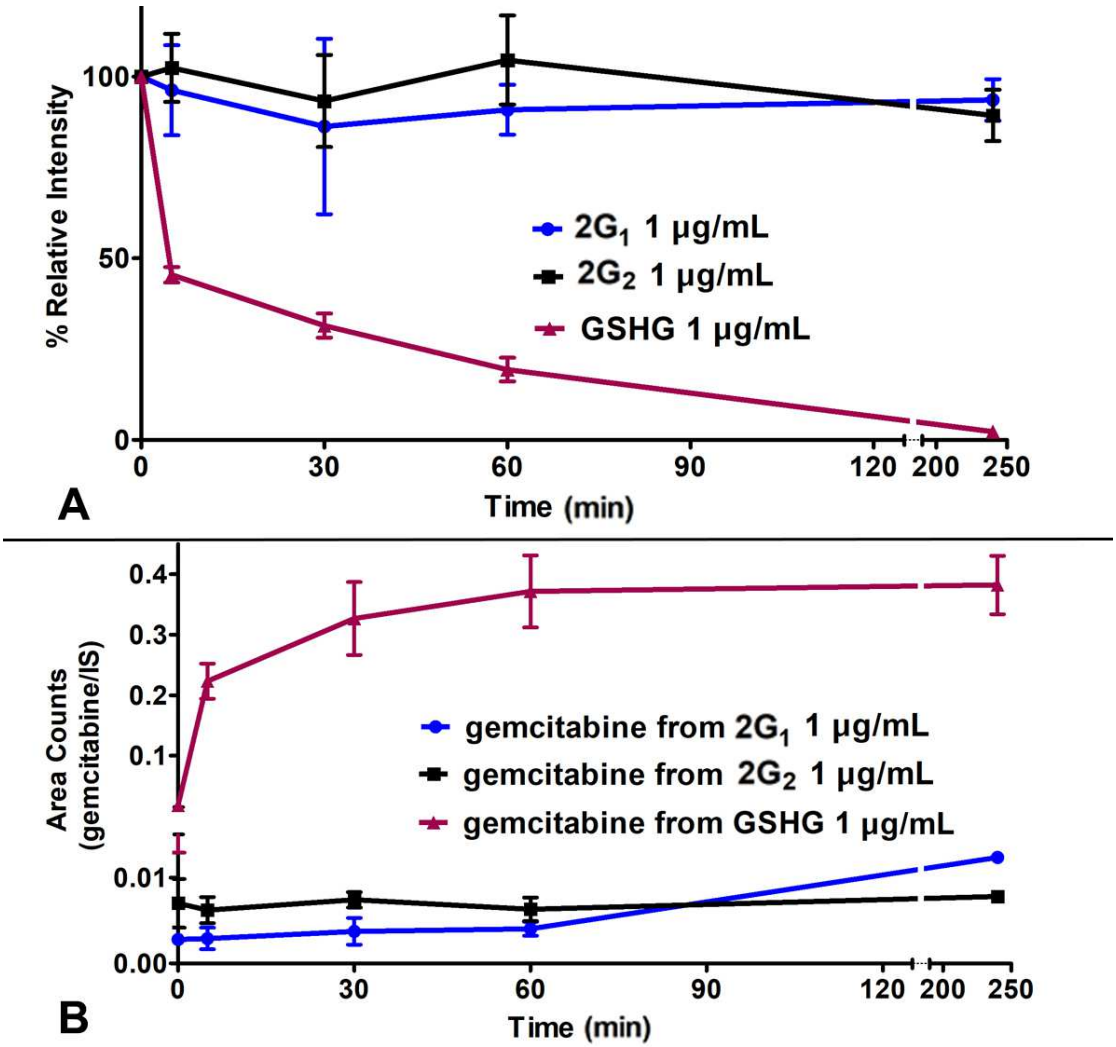

Figure 2. Stability of the three conjugates (**2G$_1$**, **2G$_2$** and **GSHG**) over time in human plasma (A) and release of gemcitabine (B).

These results are in accordance with the cell culture stability experiments presented in **Figure 1**. Similarly, **GSHG** that has the lowest stability in human plasma releases the highest amount of gemcitabine, while the other two conjugates (**2G$_1$**, **2G$_2$**) are more stable, thus resulting in reduced amounts of free gemcitabine in plasma and lower cytotoxicity.

2.6 Pharmacokinetics of 2G$_1$, 2G$_2$ and GSHG in mice.

In order to further probe the pharmacokinetic profile of the three synthesized PDCs *in vivo* we performed relevant studies in mice. Administration of the three conjugates in mice led to significantly high levels of the conjugate in blood regarding the two short-linked, via carbamate bond, analogues **2G$_1$** and **2G$_2$** (blood concentrations of at least 4

μg/mL in 15, 30 min) as shown in **Figure 3A**. In contrast, long-linked, via aminocaproic-succinic linkers, analogue **GSHG** led to low levels of the corresponding conjugate (**Figure 3A**). The high stability of **2G$_1$** and **2G$_2$** resulted in minimum levels of free gemcitabine in blood, in contrast with **GSHG** (**Figure 3B**).

In marked contrast to **2G$_1$** and **2G$_2$** blood levels in mice (4 μg/mL and 5 μg/mL, respectively in 30 min), the levels of gemcitabine in blood (approximately 3 ng/ml) were significantly low after administration of these conjugates. Administration of the same dose (10 mg/kg) of the conjugate **GSHG** has the opposite results. Its concentration in mice blood is considerably low compared to the other two conjugates, while the levels of released gemcitabine from **GSHG** were significantly higher, averaging approximately 300 ng/ml in 30 min after the administration.

Regarding the formation of the inactive metabolite of gemcitabine (dFdU), no detectable levels were observed in **2G$_1$** or **2G$_2$** samples, while for **GSHG** it averaged approximately 500 ng/mL in 1 h after the administration (**Figure 3C**).

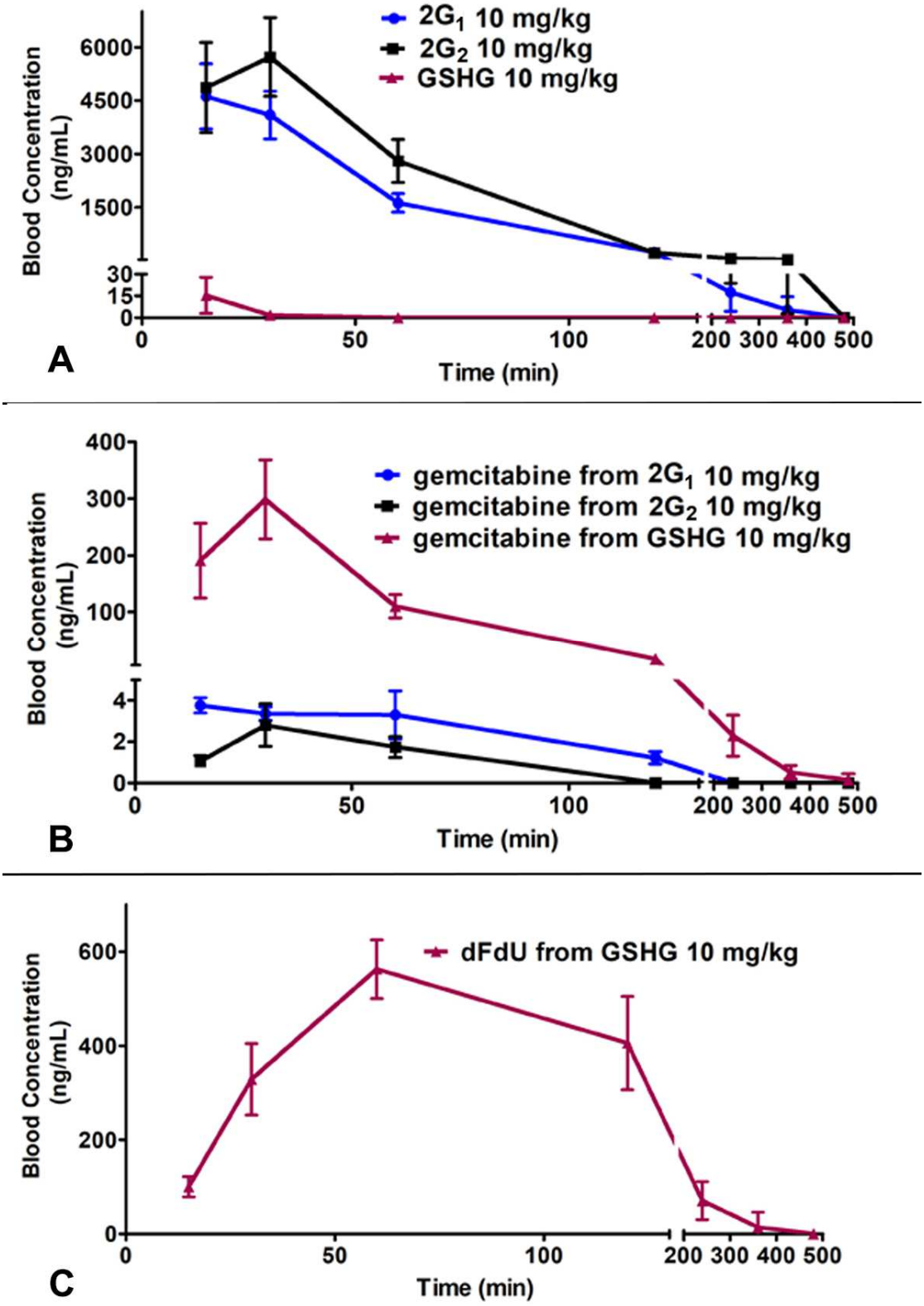

Figure 3. Pharmacokinetic evaluation of of **$2G_1$**, **$2G_2$** and **GSHG** in mice. Blood concentrations of the conjugates (A), gemcitabine (B) and dFdU (C) after 10 mg/kg IP administration of conjugate in mice.

2.7 Determination of intracellular concentrations of $2G_1$, $2G_2$ and GSHG in cancer cell line DU145.

The intracellular levels measured over time in cancer cells DU145 (**Figure 4**) for the three conjugates, indicated that **$2G_2$** achieved the highest intracellular concentration with a peak at approx. 15 ng/10^6 cells in 4 h. On the other hand, **GSHG** illustrated the smallest intracellular quantity, with a peak at 8 ng/10^6 cells. The last could be related to the fact that **GSHG** adopts the lowest binding affinity of these analogues for the GnRH-R, while **$2G_2$** possesses the highest one (as shown in **Table 3**). This trend could potentially suggest that the highest affinity of the bioconjugate to the peptide receptor could be associated with enhanced intracellular entrance, as has been also observed in former studies on GnRH-R [40, 41].

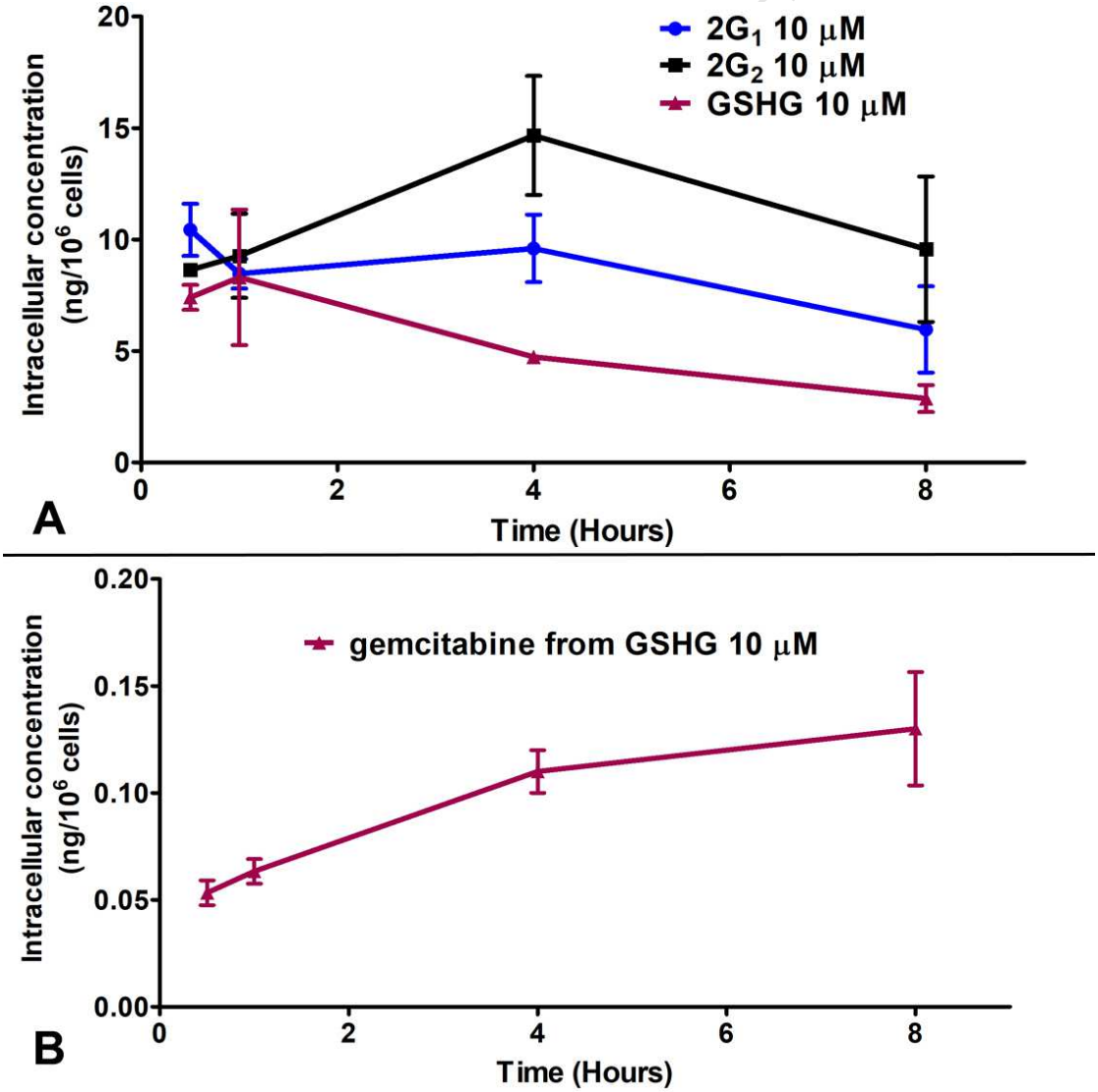

Figure 4. Intracellular levels of **$2G_1$**, **$2G_2$** and **GSHG (A)** and gemcitabine **(B)** over time after incubation of the three conjugates with DU145 cells.

Table 3. AUCs of intracellular levels of conjugates **$2G_1$**, **$2G_2$** and **GSHG** after cell uptake with DU145 cells

Compounds	$AUC_{(1\text{-}8\ hr)}$ ($ng/10^6$ cells × hr)
$2G_1$	62.8
$2G_2$	88.7
GSHG	38.6

Based on the AUC values presented in **Table 3**, **GSHG** possesses inferior cell uptake compared to conjugates **$2G_1$** and **$2G_2$**.

Incubation of **$2G_1$** and **$2G_2$** in cancer cell lines DU145 did not result in intracellular detection of gemcitabine, suggesting again that this linkage is very stable and gemcitabine was not released even after 8 hours. On the other hand, **GSHG** resulted in increasing levels of gemcitabine over time (**Figure 4B**), resulting in a relatively rapid release of the drug.

Importantly, no detectable levels of the metabolite dFdU were observed in any of the three incubations (data not shown). Although this was expected for the two short-linked conjugates due to minimum release of gemcitabine, it was surprising for the **GSHG** conjugate.

Apparently, **GSHG** has a more advantageous balance profile regarding cell uptake and stability, whereas **$2G_1$** and **$2G_2$** although enter cells more readily than **GSHG** cannot release rapidly gemcitabine, the free form of which exerts cytotoxic actions. Thus, it can be envisioned that **$2G_1$** and **$2G_2$** could be potentially utilized for long term administration of gemcitabine, while **GSHG** for short term.

3. Conclusions

Gemcitabine is a widely used anticancer nucleoside agent that possesses high toxicity against both cancer and healthy cells. Peptide-drug conjugates have emerged as a useful tool that enables the controlled release of the cytotoxic warhead at a specific site and in time- and/or quantity- controlled manner. These characteristics are based on the type of the labile linker utilized in each conjugate tethering the drug with the peptide. Herein, we report the construction, synthesis and biological evaluation of three novel gemcitabine-GnRH conjugates utilizing different linkers with the aim to provide targeted delivery of gemcitabine to the cancer tissues in due time or

sporadically. We synthesized two bioconjugates through a small carbamate linker, in the case of **$2G_1$** and **$2G_2$**, and one through a long linker which is composed of an ester and two amide bonds, in the case of **GSHG**. Utilizing the specific types of linkers, we provided PDCs with enhanced binding affinity to the GnRH-R and also, we were able to manipulate the release of native gemcitabine as monitored through our *in vivo* pharmacokinetics in mice, uptake in different cancer cell cultures, as also cell culture and human plasma stability evaluations. In addition, we achieved an enhancement of the bioavailability of the drug, especially in the cases of **$2G_1$** and **$2G_2$** which proved to be hydrolytically stable. **GSHG** on the other hand, showed rapid release of gemcitabine and consequently quite higher degradation rate, associated with reduced levels of the inactive metabolite dFdU. In conclusion, the linker tethering the cytotoxic drug and the carrier is of great significance regarding the overall bioactivity of the final conjugate, offering unique release rates. Our proposed conjugates proved to be very promising for selective drug delivery, with enhanced properties and a time-controllable release of the parent drug.

4. Experimental Section

4.1 Chemicals

Gemcitabine was purchased from Carbosynth (Compton, Berkshire, UK). HATU ((O-(7-azabenzotriazol-1-yl)- N, N, N', N'-tetramethyluronium hexafluorophosphate) and HOBt (1-hydroxybenzotriazole) were purchased from GLB (GLBiochem, China). Bis(4-nitrophenyl)carbonate, ε-aminocaproic acid and DIC (N,N'-diisopropylcarbodiimide) were purchased from Sigma Aldrich. Boc_2O (di-tert-butyldicarbonate) from Alfa Aesar (A Johnson Matthey Company, Germany). Triisopropylsilane (TIS), N, N-diisopropylethylamine (DIPEA), trifluoroacetic acid (TFA) were purchased from Merck (Darmstadt, Germany). N, N Dimethylformamide (DMF) was distilled over CaH_2 and stored under pre-activated molecular sieves 4A. Deuterated solvents were purchased from Deutero (Deutero GmBH, Kastellaun, Germany). Ammonium acetate, formic acid and 3-(4,5-dimethylthiazol-2-yl)-2,5-diphenyl-tetrazolium bromide (MTT) were purchased from Sigma-Aldrich (Sigma-Aldrich Chemie GmbH, Munich, Germany). Acetonitrile (LC-MS grade) was purchased from Fisher Scientific (Fisher Scientific, Loughborough, UK). Water (LC-MS grade) was purchased from Carlo Erba (Carlo Erba, Milan, Italy). Thin-layer

chromatography (TLC) was performed on TLC plates, silica gel coated with fluorescent indicator F254. Column chromatography was performed using SiO_2 and the appropriate elution solvent mixture as idnicated in each experimental procedure. The ^{1}H NMR and ^{13}C NMR spectra were recorded on a Bruker AV400, using DMSO-d_6 and 298 K. Chemical shifts for ^{1}H NMR spectra are reported as δ units of parts per million (ppm) and relative to the signal of DMSO-d_6 (δ 2.50 multiplet). Multiplicities are given as follows: s (singlet); d (doublet); dd (doublet of doublets); t (triplet); bs (broad singlet); m (multiplet). Coupling constants are reported as J values in Hz. HPLC was accomplished on a Shimadzu preparative liquid chromatographer, with a photodiode array detector (SPD-M20A) and an LC-8A pump. Purification by preparative RP-HPLC was conducted on an Ascentis® C18 column (25 cm × 21.2 mm) at a flow rate of 20 mL/min and 10 μm particle size as stationary phase. For the MS characterization of the synthesized compounds, the samples were injected directly to an EVOQ™ Elite ER LC-TQ system (Bruker, Germany).

4.2 Synthesis of D-Lys^{6}-GnRH-gemcitabine conjugates

D-Lys^{6}-GnRH was synthesized manually via the classic Fmoc- solid phase peptide synthesis on a Rink Amide resin (0.58 mmol/g). RP-HPLC, NMR and MS data for the syntheses of **$2G_1$**, **$2G_2$** and **GSHG** are presented in the Supporting Information (Fig. S1 – Fig. S19).

*4.2.1. 6-((tert-butoxycarbonyl)amino)hexanoic acid **(2)***

1 M aq. NaOH (0.762 mL, 0.76 mmol) was added dropwise at 0 ^{0}C to a stirring solution of **1** (100 mg, 0.76 mmol) in 10 mL Dioxane/H_2O (2/1, v/v). After 5 mins, Boc_2O (166.4 mg, 1.52 mmol) was added and the reaction was stirred at rt. Reaction was monitored via TLC (5 % methanol in CH_2Cl_2, Rf=0.32). After 3 h, the solvent was evaporated under reduced pressure. Water (5 mL) was added, pH was adjusted to pH=1 with 1 M aq. HCl and then extracted thrice with ethyl acetate (10 mL × 3). Combined organic phases were washed once with brine and dried over sodium sulphate. After filtration, the solvent was concentrated under reduced pressure to afford compound **2** (170 mg, 96.47 %) as a colorless liquid (m.p.=35-40 ^{o}C). **^{1}H-NMR of (2) (400 MHz, DMSO-d_6, 25^{o}C):** δ = 12.01 (bs, 1H), 6.78 (t, J = 5.06 Hz, 1H), 2.91 (q, J = 6.66, 6.26 Hz, 2H), 2.21 (t, J = 7.33 Hz, 2H), 1.54 - 1.47 (m, 2H), 1.43 - 1.35 (m, 2H), 1.40 (s, 9H), 1.30 - 1.22 (m, 2H) ppm; **^{13}C-NMR of (2) (400**

MHz, DMSO-d_6, 25°C): δ = 174.44 (C), 155.58 (C), 77.31 (C), 40.17 (CH_2), 33.62 (CH_2), 29.20 (CH_2), 28.27 (CH_3), 25.84 (CH_2), 24.21 (CH_2) ppm; **Mass:** ESI-MS (*m/z)* Calcd. for $C_{11}H_{21}NO_4$: 231.15, found: 254.55 $[M+Na]^+$

*4.2.2. 6-amino-N-methylhexanamide - GnRH **(3)***

DIPEA (9.7 ul, 0.055 mmol) was added dropwise under inert atmosphere to a solution of **2** (2.58 mg, 0.011 mmol) and HATU (4.18 mg, 0.011 mmol) in 3 mL anhydrous DMF. After 5 mins, a solution of D-Lys^6-GnRH (14 mg, 0.011 mmol) in 2 mL DMF was added dropwise and the resulting mixture was stirred at rt for 12h. The progress was monitored via TLC in a solvent system of n-/acetic acid/water (6/2/2, v/v), which showed the complete consumption of both starting materials (**2** and D-Lys^6-GnRH) and the formation of a new spot (Rf=0.37). DMF was evaporated under high vacuum and the residue was washed thrice with MeCN (1 mL × 3) to afford 16 mg of a white solid which was used for the next reaction (Boc- deprotection) without further purification. Boc-deprotection was performed with 2 mL of cleavage cocktail containing TFA/TIS/H_2O (9.5/0.25/0.25, v/v) at rt for 1 h. The solvent was evaporated under reduced pressure and the residue was washed thrice with cold diethyl ether (2 mL × 3) to afford compound **3** (14 mg, 91.92 %) as a white solid. **Mass:** ESI-MS (*m/z*): $[M+H]^+$ calcd. for $C_{65}H_{95}N_{19}O_{14}$: 1365.73; found: 1368.22 $[M+H]^+$, 684.71 $[M+2H]^{2+}$.

*4.2.3. 4-((5-(4-((tert-butoxycarbonyl)amino)-2-oxopyrimidin-1(2H)-yl)-3-((tert-butoxycarbonyl)oxy)-4,4-difluorotetrahydrofuran-2-yl)methoxy)-4-oxobutanoic acid **(4)***

DIPEA (0.75 mL, 4.30 mmol) was added dropwise to a stirring solution of diboc-protected gemcitabine (200 mg, 0.43 mmol) and succinic anhydride (108 mg, 1.08 mmol) in 20 mL of CH_2Cl_2. The resulting mixture was stirred at rt for 4 h (reaction monitored via TLC in solvent system CH_2Cl_2/methanol 9/1, Rf= 0.04) and then 10 mL of water were added and the mixture was lyophilized. The residue was then purified via RP-HPLC (60/40 % H_2O*TFA/MeCN*TFA to 100 % MeCN*TFA for 30 min, at 254 nm, ^tR = 11.75 min) to afford compound **4** (190 mg, 78 %) as a white solid.

^{1}H-NMR of 4 (400 MHz, DMSO-d_6, 25°C): δ = 12.31 (s, 1 H), 10.61 (s, 1 H), 8.01 (d, J = 7.6 Hz, 1 H), 7.15 (d, J = 7.6 Hz, 1 H), 6.33 (t, J = 8.7 Hz, 1 H), 5.33 (m, 1 H),

4.51 (m, 1 H), 4.48 (m, 1 H), 4.41 (m, 1 H), 2.6 (t, 2 H), 2.54 (t, 2 H), 1.50 (s, 9 H), 1.49 (s, 9 H) ppm. **^{13}C-NMR (400 MHz, DMSO-d$_6$, 25^{o}C)**: δ = 174.27 (C), 172.84 (C), 164.67 (C), 154.72 (C), 152.84 (C), 152.02 (C), 146.18 (C), 122.13 (CF_2), 96.32 (CH), 85.60 (CH), 84.81 (C), 82.32 (C), 76.91 (CH), 73.88 (CH), 63.24 (CH_2), 29.51 (CH_2), 28.66 (CH_3), 28.05 (CH_3) ppm. **Mass:** ESI-MS (*m/z)* for $C_{23}H_{30}F_2N_3O_{11}$: 563.5; found: 562.1 $[M\text{-}H^-]^-$.

4.2.4. ***GSHG***

DIPEA (10.2 ul, 0.058 mmol) was added dropwise under inert atmosphere to a stirring solution of **4** (6.6 mg, 0.011 mmol) and HATU (4.18 mg, 0.011 mmol) in 3 mL anhydrous DMF. After 5 mins, a solution of **3** (16 mg, 0.011 mmol) in 2 mL anhydrous DMF was added dropwise and the resulting mixture was stirred at rt for 12h. TLC in solvent system of n-BuOH/acetic acid/water (6/2/2, v/v) showed the complete consumption of both starting compounds **3** and **4** and the formation of a new spot (Rf=0.31). DMF was removed under high vacuum and the residue was washed thrice with MeCN (1 mL × 3) to afford 11 mg of white solid which was used for the next reaction (Boc-deprotection) without further purification. Boc-deprotection was performed with 2 mL of cleavage cocktail containing TFA/TIS/H_2O (9.5/0.25/0.25, v/v) at rt for 1 h. The solvent was evaporated under reduced pressure and the residue was washed thrice with cold diethyl ether (2 mL × 3) to afford crude **GSHG**. After RP-HPLC purification (90/10 % H_2O*TFA/MECN*TFA to 70 % H_2O*TFA for 30 min, at 214 nm, ^{t}R=23.35 min), 5 mg (24.91 %) of pure **GSHG** were obtained as a white solid. **Mass:** ESI-MS (*m/z*) calcd. for $C_{78}H_{108}F_2N_{22}O_{20}$: 1710.81 $[M+H]^+$; found: 856.3 $[M+2H]^{2+}$, 571.3 $[M+3H]^{3+}$.

*4.2.5. tert-butyl (1-(4-((tert-butoxycarbonyl)oxy)-3,3-difluoro-5-((((4-nitrophenoxy) carbonyl)oxy)methyl)tetrahydrofuran-2-yl)-2-oxo-1,2-dihydropyrimidin-4-yl)carbamate (**2a**) and tert-butyl (1-(5-(((tert-butoxycarbonyl)oxy)methyl)-3,3-difluoro-4-(((4-nitrophenoxy) carbonyl)oxy)tetrahydrofuran-2-yl)-2-oxo-1,2-dihydropyrimidin-4-yl)carbamate (**2b**)*

DIPEA (752.4 ul, 4.319 mmol) was added to a solution of **1a/2b** (50 mg, 0.107 mmol) in anhydrous MeCN (10 mL), under inert atmosphere at -10 ^{0}C (ice/acetone bath). After 5 min, a solution of Bis(4-nitrophenyl)carbonate (260.4 mg, 0.856 mmol) in 5 mL anhydrous MeCN was added dropwise and the resulting mixture was stirred at rt

The progress of the reaction was monitored via TLC in acetone/CH_2Cl_2 (1/10, v/v, Rf=0.79). After 4 h, solvent was removed under reduced pressure and the residue was purified via column chromatography (eluant: CH_2Cl_2/acetone 9/1) to afford compound **2a/2b** (60 mg, 88.58 %)/(26mg, 38.39 %) as white solids. **^{1}H-NMR of 2a (400 MHz, DMSO-d_6, 25^{o}C):**δ = 10.58 (s, 1 H), 8.33 (d, J = 9.14 Hz, 2H), 8.02 (d, J = 7.67 Hz, 1H), 7.59 (d, J = 9.14 Hz, 2H), 7.08 (d, J = 7.55 Hz, 1H), 6.31 (t, J = 8.69 Hz, 1H), 5.46 - 5.36 (m, 1H), 4.69 - 4.67 (m, 1H), 4.64 - 4.56 (m, 2H), 1.46 (s, 9H), 1.45 (s, 9H) ppm; **^{13}C-NMR of 2a (400 MHz, DMSO-d_6, 25^{o}C):**δ = 163.84 (C), 155.17 (C), 153.80 (C), 151.86 (C), 151.73 (C), 151.11 (C), 145.60 (CH), 145.28 (C), 126.20 (C), 125.45 (CH), 122.62 (CH), 115.83 (C), 95.35 (CH), 83.95 (C), 81.45 (C), 75.69 (CH), 72.86 (CH), 67.13 (CH_2), 27.73 (CH_3), 27.13 (CH_3) ppm; **Mass:** ESI-MS (*m/z)* calcd. for $C_{26}H_{30}F_2N_4O_{12}$: 628.18 $[M+H]^+$, found: 629.93 $[M+H]^+$.

^{1}H-NMR of 2b (400 MHz, DMSO-d_6, 25^{o}C):δ = 10.60 (s, 1 H), 8.35 (d, J = 9.15 Hz, 2H), 8.04 (d, J = 7.7 Hz, 1H), 7.64 (d, J = 9.15Hz, 2H), 7.09 (d, J = 7.65 Hz, 1H), 6.35 (t, J = 8.56 Hz, 1H), 5.52 (m, 1H), 4.62 - 4.54 (m, 2H), 4.45 - 4.35 (m, 1H), 1.46 (s, 9H), 1.42 (s, 9H) ppm; **^{13}C-NMR of 2b (400 MHz, DMSO-d_6, 25^{o}C):** δ = 163.87 (C), 154.82 (C), 153.82 (C), 152.53 (C), 151.87 (C), 150.74 (C), 145.51 (CH), 126.19 (C), 125.56 (CH), 122.45 (CH), 115.80 (C), 95.30 (CH), 82.23 (CH), 81.45 (C), 75.77 (C), 74.60 (CH), 72.49 (CH), 65.24 (CH_2), 28.74 (CH_3), 27.29 (CH_3) ppm; **Mass:** ESI- MS (*m/z)* calcd. for $C_{26}H_{30}F_2N_4O_{12}$: 628.18 $[M+H]^+$, found: 629.87 $[M+H]^+$.

4.2.6. ***2G$_1$*** *and* ***2G$_2$***

DIPEA (8.34 ul, 0.047 mmol) was added dropwise to a solution of GnRH (20 mg, 0.01596 mmol) in 2 mL anhydrous DMF under inert atmosphere at 0 ^{o}C. After 5 min, a solution of **2a/2b** (10 mg, 0.015 mmol) in anhydrous 1 mL DMF, was added dropwise and the resulting mixture was stirred at rt. The reaction was monitored via TLC using acetone/CH_2Cl_2 1/9 and then n-BuOH/AcOH/H_2O (6/2/2, v/v, Rf=0.33). After 12 h, solvent was removed under high vacuum and the residue was washed twice with acetonitrile (2 mL × 2). The residues were dissolved in 3 mL of cleavage cocktail (TFA/TIS/ H_2O, 9.5/0.25/0.25, v/v) at 0 ^{o}C and stirred at rt for 12 h. Solvent was evaporated under reduced pressure and the residue was washed thrice with cold diethyl ether (2 mL × 3). Crude compounds were purified with semi preparative RP-HPLC (90/10 % H_2O*TFA/MeCN*TFA to 70 % H_2O*TFA for 30 min, at 214 nm,

$^{t}R_{2G1}$=29.50 min and $^{t}R_{2G2}$=28.50 min) and the fractions were lyophilized to afford compound **$2G_1$/$2G_2$** (12.5 mg, 50.81 %) / (12 mg, 48.78 %).

Mass of $2G_1$: ESI-MS (*m/z*): calcd. for C_{69} $H_{93}F_2N_4O_{18}$: 1541.8 $[M+H]^+$, found: 771.9 $[M+2H]^{2+}$; 514.9 $[M+3H]^{3+}$.

Mass of $2G_2$: ESI-MS (m/z): calcd. for C_{69} $H_{93}F_2N_4O_{18}$: 1541.8 $[M+H]^+$, found: 771.8 $[M+2H]^{2+}$; 514.9 $[M+3H]^{3+}$.

4.3 Characterization and quantitative analysis of GnRH-gemcitabine conjugates, gemcitabine and dFdU by Liquid Chromatography-Mass Spectrometry (LC-MS/MS)

For the identification and quantification of gemcitabine, dFdU and GnRH-gemcitabine conjugates, LC-MS/MS methodologies were developed and validated as described previously [42]. HPLC was performed using a Dionex Ultimate 3000 system (Dionex Corporation, Germering, Germany) equipped with three pumps (two for nano and one for micro LC), a temperature-controlled column compartment and an autosampler. A C18 column (Agilent, ZORBAX Eclipse, 4.6 x 150 mm, 5 μM) was used at a flow rate of 1 mL/min for the separation of analytes of interest. The mobile phase consisted of A: 10% MeCN, 90% water, 2 mM ammonium acetate, and 0.1% FA and B: 90% MeCN, 10% water, 2 mM ammonium acetate, and 0.1% FA. Mass spectrometry was performed on an API 4000 QTRAP LC-MS/MS system fitted with a TurboIonSpray source and a hybrid triple quadrupole/linear ion trap mass spectrometer (Applied Biosystems, Concord, Ontario, Canada).

4.4 Binding to the human GnRH-R

Radioiodination of D-Tyr^6-His^5-GnRH, preparation of membrane homogenates from HEK 293 cells stably expressing the GnRH-R and binding of the GnRH-gemcitabine conjugates to the human GnRH-R was performed as described before [43, 44]. In brief, aliquots of diluted membrane suspension (50 μL) were added into tubes containing buffer B (25 mM HEPES containing 1 mM $CaCl_2$, 10 mM $MgCl_2$, 0.5% BSA, pH 7.4 at 4 ^{o}C) and 100,000-120,000 cpm [^{125}I]-D-Tyr^6-His^5-GnRH with or without increasing concentrations of GnRH-gemcitabine conjugates in a final volume of 0.2 mL. The mixtures were incubated at 4 °C for 16-19 h and then filtered using a Brandel cell harvester through Whatman GF/C glass fiber filters, presoaked for 1-2 h in 0.5% polyethylenimine at 4 °C. The filters were washed four times with 1.5 mL of

ice-cold 50 mM Tris-HCl, pH 7.4 at 4 ^{o}C. Filters were assessed for radioactivity in a gamma counter (LKB Wallac 1275 minigamma, 80% efficiency). The amount of membrane used was adjusted to ensure that the specific binding was always equal to or less than 10% of the total concentration of the added radioligand. Specific [^{125}I]-D-Tyr^{6}-His^{5}-GnRH binding was defined as total binding less nonspecific binding in the presence of 1000 nM triptorelin (Bachem, Germany). Data for competition binding were analyzed by nonlinear regression analysis, using GraphPad Prism 4.0 (GraphPad Software, San Diego, CA). IC_{50} values were obtained by fitting the data from competition studies to a one-site competition model.

4.5 Cell Cultures

The androgen-independent CaP cell lines DU145, PC3, the triple negative breast cancer MDA-MB-231 and the luminal A breast cancer MCF-7 were used in this study. Cells were maintained in RPMI (DU145, PC3, MDA-MB-231) or DMEM (MCF7) medium, containing glutamine and supplemented with 10% Fetal Bovine Serum (FBS), penicillin (100 U/mL) and streptomycin (100 mg/mL) at 37 °C and 5% CO_2.

4.6 Cell Growth Assay

Cells were plated at a density of 5 x 10^3 cells per well on 96-well plates. After 24 h incubation (37 ^{o}C, 5% CO_2), the cell medium was removed, and compounds were added at selected concentrations (10-40,000 nM), followed by incubation for 72 h. The medium was then removed and the MTT solution (0.3 mg/mL in PBS) was added to cells for 3 h, after which the MTT solution was removed and the formazan crystals were dissolved in 100 µL DMSO. The optical density was measured at 570 nm and a reference wavelength of 690 nm using an absorbance microplate reader (SpectraMax 190, Molecular Devices, Sunnyvale, CA, USA). The 50% cytostatic concentration (IC50) was calculated based on a four-parameter logistic equation using SigmaPlot 12 software (Systat Software, San Jose, CA, USA). Each point was the result of three experiments performed in triplicate.

4.7 Determination of intracellular concentrations of conjugates, gemcitabine and dFdU

Cells (DU145) were plated in 6-well plates at a density of 2 x 10^6 cells/well. Cells were then incubated with **$2G_1$**, **$2G_2$**, **GSHG** or gemcitabine (10 µM) for selected time

points (1 h, 4 h, 8 h). Incubations were terminated by removing the medium and washing the cells twice with ice cold PBS to remove unbound gemcitabine or the conjugates. The cells were then lysed by adding an ice-cold solution of MeCN-Water (3:2) and scraping the cell monolayer. Samples were subsequently vortexed, sonicated and centrifuged for three minutes at 16,060 g (Heraeus Biofuge Pico microcentrifuge, Thermo Scientific, Bonn, Germany). The supernatants were collected, evaporated and stored at -20 ^{o}C until the day of analysis. Intracellular accumulation of the conjugates, gemcitabine and dFdU was determined by LC-MS/MS analysis using a stable internal standard as well as gemcitabine and dFdU standards for the construction of analytical standard curves.

4.8 In vitro stability in cell culture

$2G_1$, **$2G_2$** and **GSHG** 1 μM were incubated in cell culture medium (RPMI, 10%FBS, 1 % P/S) at 37 ^{o}C. Samples (triplicates of 40 μL) were collected at selected time points (t= 0, 1, 2, 4, 8, 24, 48, 72 hours) and were stored at -80 ^{o}C after mixing with 160 μL of initial mobile phase (90 % H_2O, 10 % MeCN, 2 mM ammonium acetate, 0.1 % formic acid). Samples were analyzed using LC-MS/MS.

4.9 In vitro stability in human plasma

1 μg/mL of either **$2G_1$**, **$2G_2$** or **GSHG** were incubated in human plasma. Samples (triplicates of 50 μL) were collected at selected time points (t= 0, 0.08, 0.5, 1, 4 hours) were stored at -80 ^{o}C after mixing with 150 μL acetonitrile. Samples were then extracted using protein precipitation and analyzed using LC-MS/MS.

4.10 In vivo pharmacokinetics

All animal procedures were approved by the Project Evaluation Committee of the Institution and the competent Veterinary Service of the Prefecture of Athens, in accordance to the National legal framework on the protection of animals used for scientific purposes (Presidential Decree 56/2013 in harmonization to the European Directive 2010/63). For pharmacokinetic studies, animals at the age of 8-12 weeks were weighed and fasted overnight before dosing (n = 5 per group, male C57BL/6N inbred strain obtained from Charles River, Calco, Italy). Dosing solutions of GnRH conjugates (10 mg/kg or 6.3 μmol/kg) or an equimolar dose of gemcitabine (1.65 mg/kg) in saline were administered intraperitoneally (IP). A serial tail bleeding

protocol was used for the collection of blood samples. Blood samples (10 μL) were collected at selected time points (0.25 h, 0.5 h, 1 h, 2 h, 4 h, 6 h, 8 h) in tubes containing 40 μL citric acid (0.1 M, pH 4.5) and stored at -80 °C until sample extraction. Samples were prepared for quantification by protein precipitation and evaporation. **$2G_1$**, **$2G_2$**, **GSHG**, gemcitabine and dFdU were quantified by LC-MS/MS analysis.

4.11 Statistical Analysis

The results presented herein are expressed as mean ± SD. Statistical analyses were performed by the SigmaPlot 12 software. Statistical significance was determined by using Student's t test.

Supporting information

NMR, MS and HPLC spectra for all the synthesized compounds are presented in the Supporting Information (**Figure S1-S19**).

Acknowledgments

This work was co-financed by the European Union (European Social Fund ESF) and reek national funds through the Operational Program "Education and Lifelong Learning" of the National Strategic Reference Framework (NSRF) – Research Funding Program: ARISTEIA II [grant number: 5199]. Also, this research was co-financed by Greece and the European Union (European Social Fund- ESF) through the Operational Programme "Human Resources Development, Education and Lifelong Learning 2014-2020" in the context of the project "Strengthening Human Resources Research Potential via Doctorate Research – 2nd Cycle" (MIS 5000432).

References

[1] A.K. Mitra, V. Agrahari, A. Mandal, K. Cholkar, C. Natarajan, S. Shah, M. Joseph, H.M. Trinh, R. Vaishya, X. Yang, Y. Hao, V. Khurana, D. Pal, Novel delivery approaches for cancer therapeutics, Journal of Controlled Release, 219 (2015) 248-268.

[2] O. Argyros, T. Karampelas, X. Asvos, A. Varela, N. Sayyad, A. Papakyriakou, C.H. Davos, A.G. Tzakos, D. Fokas, C. Tamvakopoulos, Peptide-Drug Conjugate GnRH-Sunitinib Targets Angiogenesis Selectively at the Site of Action to Inhibit Tumor Growth, Cancer research, 76 (2016) 1181-1192.

[3] T. Karampelas, O. Argyros, N. Sayyad, K. Spyridaki, C. Pappas, K. Morgan, G. Kolios, R.P. Millar, G. Liapakis, A.G. Tzakos, D. Fokas, C. Tamvakopoulos, GnRH-Gemcitabine conjugates for the treatment of androgen-independent prostate cancer: pharmacokinetic enhancements combined with targeted drug delivery, Bioconjugate chemistry, 25 (2014) 813-823.
[4] E.I. Vrettos, G. Mezo, A.G. Tzakos, On the design principles of peptide-drug conjugates for targeted drug delivery to the malignant tumor site, Beilstein journal of organic chemistry, 14 (2018) 930-954.
[5] M.A. El Mubarak, I. Leontari, G. Efstathia, E.I. Vrettos, A.K. Shaikh, S.E. Konstantinos, C. Danika, H.P. Kalofonos, A.G. Tzakos, G.B. Sivolapenko, Development of a novel conjugatable sunitinib analogue validated through in vitro and in vivo preclinical settings, Journal of chromatography. B, Analytical technologies in the biomedical and life sciences, 1092 (2018) 515-523.
[6] M.J. Akhtar, M. Ahamed, H.A. Alhadlaq, S.A. Alrokayan, S. Kumar, Targeted anticancer therapy: overexpressed receptors and nanotechnology, Clinica chimica acta; international journal of clinical chemistry, 436 (2014) 78-92.
[7] G.A. Gonzalez-Conchas, L. Rodriguez-Romo, D. Hernandez-Barajas, J.F. Gonzalez-Guerrero, I.A. Rodriguez-Fernandez, A. Verdines-Perez, A.J. Templeton, A. Ocana, B. Seruga, I.F. Tannock, E. Amir, F.E. Vera-Badillo, Epidermal growth factor receptor overexpression and outcomes in early breast cancer: A systematic review and a meta-analysis, Cancer Treatment Reviews, 62 (2018) 1-8.
[8] J.B. Engel, H.R. Tinneberg, F.G. Rick, E. Berkes, A.V. Schally, Targeting of Peptide Cytotoxins to LHRH Receptors For Treatment of Cancer, Current drug targets, 17 (2016) 488-494.
[9] A. Nagy, A.V. Schally, P. Armatis, K. Szepeshazi, G. Halmos, M. Kovacs, M. Zarandi, K. Groot, M. Miyazaki, A. Jungwirth, J. Horvath, Cytotoxic analogs of luteinizing hormone-releasing hormone containing doxorubicin or 2-pyrrolinodoxorubicin, a derivative 500-1000 times more potent, Proceedings of the National Academy of Sciences, 93 (1996) 7269-7273.
[10] Y. Wang, A.G. Cheetham, G. Angacian, H. Su, L. Xie, H. Cui, Peptide-drug conjugates as effective prodrug strategies for targeted delivery, Adv Drug Deliv Rev, 110-111 (2017) 112-126.
[11] L. Ma, C. Wang, Z. He, B. Cheng, L. Zheng, K. Huang, Peptide-Drug Conjugate: A Novel Drug Design Approach, Current medicinal chemistry, 24 (2017) 3373-3396.
[12] V. Kushwah, S.S. Katiyar, A.K. Agrawal, I. Saraf, I.P. Singh, D.A. Lamprou, R.C. Gupta, S. Jain, Implication of linker length on cell cytotoxicity, pharmacokinetic and toxicity profile of gemcitabine-docetaxel combinatorial dual drug conjugate, International journal of pharmaceutics, 548 (2018) 357-374.
[13] K.C. Cundy, S. Sastry, W. Luo, J. Zou, T.L. Moors, D.M. Canafax, Clinical pharmacokinetics of XP13512, a novel transported prodrug of gabapentin, Journal of clinical pharmacology, 48 (2008) 1378-1388.
[14] N. Masuda, S.J. Lee, S. Ohtani, Y.H. Im, E.S. Lee, I. Yokota, K. Kuroi, S.A. Im, B.W. Park, S.B. Kim, Y. Yanagita, S. Ohno, S. Takao, K. Aogi, H. Iwata, J. Jeong, A. Kim, K.H. Park, H. Sasano, Y. Ohashi, M. Toi, Adjuvant Capecitabine for Breast Cancer after Preoperative Chemotherapy, The New England journal of medicine, 376 (2017) 2147-2159.
[15] M.-L. Ţînţaş, V. Gembus, F. Alix, A. Barré, G. Coadou, L. Truong, M. Sebban, C. Papamicaël, H. Oulyadi, V. Levacher, Rational design of carbamate-based dual binding site and central AChE inhibitors by a “biooxidisable” prodrug approach:

Synthesis, in vitro evaluation and docking studies, European Journal of Medicinal Chemistry, 155 (2018) 171-182.
[16] A.K. Ghosh, M. Brindisi, Organic carbamates in drug design and medicinal chemistry, Journal of medicinal chemistry, 58 (2015) 2895-2940.
[17] Y. Gilad, E. Noy, H. Senderowitz, A. Albeck, M.A. Firer, G. Gellerman, Synthesis, biological studies and molecular dynamics of new anticancer RGD-based peptide conjugates for targeted drug delivery, Bioorganic & Medicinal Chemistry, 24 (2016) 294-303.
[18] Y. Li, Y. Wang, R. Zhang, C. Liu, Y. Wei, J. Sun, Z. He, Y. Xu, T. Zhang, Improving the oral bioavailability of tapentadol via a carbamate prodrug approach: synthesis, bioactivation, and pharmacokinetics, Drug delivery and translational research, 8 (2018) 1335-1344.
[19] M.V. Chatziathanasiadou, E.G. Geromichalou, N. Sayyad, E.I. Vrettos, A. Katsikoudi, E. Stylos, S. Bellou, G.D. Geromichalos, A.G. Tzakos, Amplifying and broadening the cytotoxic profile of quercetin in cancer cell lines through bioconjugation, Amino acids, 50 (2018) 279-291.
[20] T.F. Kellici, M.V. Chatziathanasiadou, M.S. Lee, N. Sayyad, E.G. Geromichalou, E.I. Vrettos, A.D. Tsiailanis, S.W. Chi, G.D. Geromichalos, T. Mavromoustakos, A.G. Tzakos, Rational design and structure-activity relationship studies of quercetin-amino acid hybrids targeting the anti-apoptotic protein Bcl-xL, Organic & biomolecular chemistry, 15 (2017) 7956-7976.
[21] N.A. Thiele, J. Kärkkäinen, K.B. Sloan, J. Rautio, K.M. Huttunen, Secondary carbamate linker can facilitate the sustained release of dopamine from brain-targeted prodrug, Bioorg Med Chem Lett, 28 (2018) 2856-2860.
[22] A. Mattarei, M. Azzolini, M. La Spina, M. Zoratti, C. Paradisi, L. Biasutto, Amino Acid Carbamates As Prodrugs Of Resveratrol, 5 (2015) 15216.
[23] A. Primikyri, N. Sayyad, G. Quilici, E.I. Vrettos, K. Lim, S.W. Chi, G. Musco, I.P. Gerothanassis, A.G. Tzakos, Probing the interaction of a quercetin bioconjugate with Bcl-2 in living human cancer cells with in-cell NMR spectroscopy, FEBS letters, 592 (2018) 3367-3379.
[24] L.P. Jordheim, D. Durantel, F. Zoulim, C. Dumontet, Advances in the development of nucleoside and nucleotide analogues for cancer and viral diseases, Nat Rev Drug Discov, 12 (2013) 447-464.
[25] J. Carmichael, The role of gemcitabine in the treatment of other tumours, British Journal of Cancer, 78 (1998) 21-25.
[26] M. Gusella, F. Pasini, C. Bolzonella, S. Meneghetti, C. Barile, A. Bononi, S. Toso, D. Menon, G. Crepaldi, Y. Modena, L. Stievano, R. Padrini, Equilibrative nucleoside transporter 1 genotype, cytidine deaminase activity and age predict gemcitabine plasma clearance in patients with solid tumours, British journal of clinical pharmacology, 71 (2011) 437-444.
[27] E. Mini, S. Nobili, B. Caciagli, I. Landini, T. Mazzei, Cellular pharmacology of gemcitabine, Annals of Oncology, 17 (2006) v7-v12.
[28] L. de Sousa Cavalcante, G. Monteiro, Gemcitabine: metabolism and molecular mechanisms of action, sensitivity and chemoresistance in pancreatic cancer, European journal of pharmacology, 741 (2014) 8-16.
[29] D.R. Rauchwerger, P.S. Firby, D.W. Hedley, M.J. Moore, Equilibrative-sensitive nucleoside transporter and its role in gemcitabine sensitivity, Cancer research, 60 (2000) 6075-6079.
[30] J. Spratlin, R. Sangha, D. Glubrecht, L. Dabbagh, J.D. Young, C. Dumontet, C. Cass, R. Lai, J.R. Mackey, The absence of human equilibrative nucleoside transporter

1 is associated with reduced survival in patients with gemcitabine-treated pancreas adenocarcinoma, Clinical cancer research : an official journal of the American Association for Cancer Research, 10 (2004) 6956-6961.
[31] B. Hryciuk, B. Szymanowski, A. Romanowska, E. Salt, B. Wasąg, B. Grala, J. Jassem, R. Duchnowska, Severe acute toxicity following gemcitabine administration: A report of four cases with cytidine deaminase polymorphisms evaluation, Oncology letters, 15 (2018) 1912-1916.
[32] S.A. Veltkamp, J.H. Beijnen, J.H. Schellens, Prolonged versus standard gemcitabine infusion: translation of molecular pharmacology to new treatment strategy, The oncologist, 13 (2008) 261-276.
[33] Y. Zhou, Q. Chang, W. Wang, X. Zhang, F. Zhou, J. Sun, G. Wang, Y. Peng, Sensitive analysis and pharmacokinetic study of a novel gemcitabine carbamate prodrug and its active metabolite gemcitabine in rats using LC-ESI-MS/MS, Journal of chromatography. B, Analytical technologies in the biomedical and life sciences, 1083 (2018) 249-257.
[34] H. Zhang, K. Wang, K. Na, D. Li, Z. Li, D. Zhao, L. Zhong, M. Wang, L. Kou, C. Luo, H. Zhang, Q. Kan, H. Ding, Z. He, J. Sun, Striking a Balance between Carbonate/Carbamate Linkage Bond- and Reduction-Sensitive Disulfide Bond-Bearing Linker for Tailored Controlled Release: In Situ Covalent-Albumin-Binding Gemcitabine Prodrugs Promote Bioavailability and Tumor Accumulation, Journal of medicinal chemistry, 61 (2018) 4904-4917.
[35] J.T. Weiss, J.C. Dawson, C. Fraser, W. Rybski, C. Torres-Sanchez, M. Bradley, E.E. Patton, N.O. Carragher, A. Unciti-Broceta, Development and bioorthogonal activation of palladium-labile prodrugs of gemcitabine, Journal of medicinal chemistry, 57 (2014) 5395-5404.
[36] W.E.K. Oskar Keller, Gert van Look, Gernot Wersin, tert-BUTOXYCARBONYLATION OF AMINO ACIDS AND THEIR DERIVATIVES: N-tert-BUTOXYCARBONYL-l-PHENYLALANINE, Organic Syntheses, (1985).
[37] E.I. Vrettos, N. Sayyad, E.M. Mavrogiannaki, E. Stylos, A.D. Kostagianni, S. Papas, T. Mavromoustakos, V. Theodorou, A.G. Tzakos, Unveiling and tackling guanidinium peptide coupling reagent side reactions towards the development of peptide-drug conjugates, RSC Advances, 7 (2017) 50519-50526.
[38] Z. Guo Zw, J.M. Gallo, Selective Protection of 2',2'-Difluorodeoxycytidine (Gemcitabine), The Journal of organic chemistry, 64 (1999) 8319-8322.
[39] X. Peng, B.I. Knapp, J.M. Bidlack, J.L. Neumeyer, High-affinity carbamate analogues of morphinan at opioid receptors, Bioorganic & medicinal chemistry letters, 17 (2007) 1508-1511.
[40] H. Guo, J. Lu, H. Hathaway, M.E. Royce, E.R. Prossnitz, Y. Miao, Synthesis and evaluation of novel gonadotropin-releasing hormone receptor-targeting peptides, Bioconjugate chemistry, 22 (2011) 1682-1689.
[41] M. Schottelius, S. Berger, T. Poethko, M. Schwaiger, H.J. Wester, Development of novel 68Ga- and 18F-labeled GnRH-I analogues with high GnRHR-targeting efficiency, Bioconjugate chemistry, 19 (2008) 1256-1268.
[42] Z.D. Sofianos, T. Katsila, N. Kostomitsopoulos, V. Balafas, J. Matsoukas, T. Tselios, C. Tamvakopoulos, In vivo evaluation and in vitro metabolism of leuprolide in mice--mass spectrometry-based biomarker measurement for efficacy and toxicity, Journal of mass spectrometry : JMS, 43 (2008) 1381-1392.
[43] D. Laimou, T. Katsila, J. Matsoukas, A. Schally, K. Gkountelias, G. Liapakis, C. Tamvakopoulos, T. Tselios, Rationally designed cyclic analogues of luteinizing

hormone-releasing hormone: enhanced enzymatic stability and biological properties, European journal of medicinal chemistry, 58 (2012) 237-247.
[44] T. Katsila, E. Balafas, G. Liapakis, P. Limonta, M. Montagnani Marelli, K. Gkountelias, T. Tselios, N. Kostomitsopoulos, J. Matsoukas, C. Tamvakopoulos, Evaluation of a stable gonadotropin-releasing hormone analog in mice for the treatment of endocrine disorders and prostate cancer, The Journal of pharmacology and experimental therapeutics, 336 (2011) 613-623.